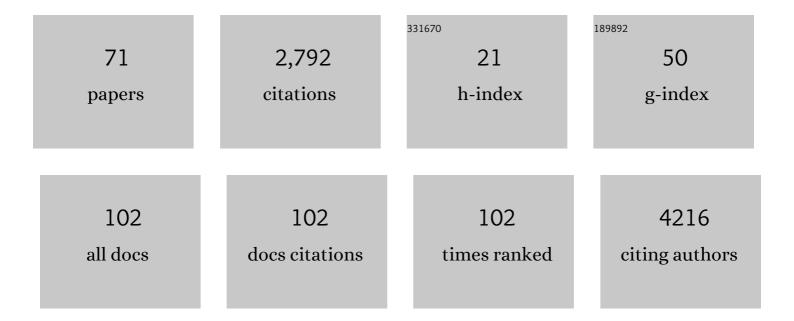
Constantino-Carlos Reyes-Aldasoro

List of Publications by Year in descending order

Source: https://exaly.com/author-pdf/6924967/publications.pdf

Version: 2024-02-01



#	Article	IF	CITATIONS
1	Automatic Gemstone Classification Using Computer Vision. Minerals (Basel, Switzerland), 2022, 12, 60.	2.0	20
2	A Novel Focal Phi Loss for Power Line Segmentation with Auxiliary Classifier U-Net. Sensors, 2021, 21, 2803.	3.8	23
3	Volumetric Semantic Instance Segmentation of the Plasma Membrane of HeLa Cells. Journal of Imaging, 2021, 7, 93.	3.0	4
4	Classification and Visualisation of Normal and Abnormal Radiographs; A Comparison between Eleven Convolutional Neural Network Architectures. Sensors, 2021, 21, 5381.	3.8	16
5	Detection of Pitt–Hopkins Syndrome Based on Morphological Facial Features. Applied Sciences (Switzerland), 2021, 11, 12086.	2.5	Ο
6	Semantic segmentation of HeLa cells: An objective comparison between one traditional algorithm and four deep-learning architectures. PLoS ONE, 2020, 15, e0230605.	2.5	15
7	Geometric semi-automatic analysis of radiographs of Colles' fractures. PLoS ONE, 2020, 15, e0238926.	2.5	7
8	Morphological Estimation of Cellularity on Neo-Adjuvant Treated Breast Cancer Histological Images. Journal of Imaging, 2020, 6, 101.	3.0	3
9	Prophase-Specific Perinuclear Actin Coordinates Centrosome Separation and Positioning to Ensure Accurate Chromosome Segregation. Cell Reports, 2020, 31, 107681.	6.4	24
10	Experimental Assessment of Color Deconvolution and Color Normalization for Automated Classification of Histology Images Stained with Hematoxylin and Eosin. Cancers, 2020, 12, 3337.	3.7	17
11	Cell Tracking Profiler: a user-driven analysis framework for evaluating 4D live cell imaging data. Journal of Cell Science, 2020, 133, .	2.0	7
12	Comparative Study of Contact Repulsion in Control and Mutant Macrophages Using a Novel Interaction Detection. Journal of Imaging, 2020, 6, 36.	3.0	0
13	A Machine Learning Approach for Colles' Fracture Treatment Diagnosis. Communications in Computer and Information Science, 2020, , 319-330.	0.5	Ο
14	Radiography Classification: A Comparison between Eleven Convolutional Neural Networks. , 2020, , .		2
15	Texture Segmentation: An Objective Comparison between Five Traditional Algorithms and a Deep-Learning U-Net Architecture. Applied Sciences (Switzerland), 2019, 9, 3900.	2.5	16
16	Segmentation and Modelling of the Nuclear Envelope of HeLa Cells Imaged with Serial Block Face Scanning Electron Microscopy. Journal of Imaging, 2019, 5, 75.	3.0	17
17	β-glucan–dependent shuttling of conidia from neutrophils to macrophages occurs during fungal infection establishment. PLoS Biology, 2019, 17, e3000113.	5.6	20
18	Predicting survival from colorectal cancer histology slides using deep learning: A retrospective multicenter study. PLoS Medicine, 2019, 16, e1002730.	8.4	563

#	Article	IF	CITATIONS
19	Macrosight: A Novel Framework to Analyze the Shape and Movement of Interacting Macrophages Using Matlab®. Journal of Imaging, 2019, 5, 17.	3.0	3
20	Visualisation and Analysis of Speech Production with Electropalatography. Journal of Imaging, 2019, 5, 40.	3.0	6
21	Effect of Viscosity and Speed on Oil Cavitation Development in a Single Piston-Ring Lubricant Assembly. Lubricants, 2019, 7, 88.	2.9	12
22	Large-scale database mining reveals hidden trends and future directions for cancer immunotherapy. Oncolmmunology, 2018, 7, e1444412.	4.6	11
23	Quantitative MRI Brain Studies in Mild Cognitive Impairment and Alzheimer's Disease: A Methodological Review. IEEE Reviews in Biomedical Engineering, 2018, 11, 97-111.	18.0	80
24	Segmentation and Shape Analysis of Macrophages Using Anglegram Analysis. Journal of Imaging, 2018, 4, 2.	3.0	8
25	Hippocampal and entorhinal cortex volume changes in Alzheimer's disease patients and mild cognitive impairment subjects. , 2018, , .		1
26	Shape analysis and tracking of migrating macrophages. , 2018, , .		3
27	Analysis of the Symmetry of Electrodes for Electropalatography with Cone Beam CT Scanning. Communications in Computer and Information Science, 2018, , 130-139.	0.5	1
28	Automated Segmentation of HeLa Nuclear Envelope from Electron Microscopy Images. Communications in Computer and Information Science, 2018, , 241-250.	0.5	3
29	A hybrid energy model for region based curve evolution – Application to CTA coronary segmentation. Computer Methods and Programs in Biomedicine, 2017, 144, 189-202.	4.7	7
30	An objective comparison of cell-tracking algorithms. Nature Methods, 2017, 14, 1141-1152.	19.0	399
31	Framework for detection and localization of coronary non-calcified plaques in cardiac CTA using mean radial profiles. Computers in Biology and Medicine, 2017, 89, 84-95.	7.0	20
32	The proportion of cancer-related entries in PubMed has increased considerably; is cancer truly "The Emperor of All Maladies�. PLoS ONE, 2017, 12, e0173671.	2.5	21
33	Improved CTA Coronary Segmentation with a Volume-Specific Intensity Threshold. Communications in Computer and Information Science, 2017, , 207-218.	O.5	0
34	Topological Analysis of the Vasculature ofÂAngiopoietin-Expressing Tumours Through Scale-Space Tracing. Communications in Computer and Information Science, 2017, , 285-296.	0.5	0
35	Segmentation of Overlapping Macrophages Using Anglegram Analysis. Communications in Computer and Information Science, 2017, , 792-803.	0.5	0
36	Maternal Hyperleptinemia Is Associated with Male Offspring's Altered Vascular Function and Structure in Mice. PLoS ONE, 2016, 11, e0155377.	2.5	15

#	Article	IF	CITATIONS
37	Arterial Stiffening in Western Diet-Fed Mice Is Associated with Increased Vascular Elastin, Transforming Growth Factor-β, and Plasma Neuraminidase. Frontiers in Physiology, 2016, 7, 285.	2.8	33
38	An Overview of Quantitative Magnetic Resonance Imaging Analysis Studies in the Assessment of Alzheimer's Disease. IFMBE Proceedings, 2016, , 281-286.	0.3	2
39	Continuous representation of tumor microvessel density and detection of angiogenic hotspots in histological whole-slide images. Oncotarget, 2015, 6, 19163-19176.	1.8	53
40	Whole cell tracking through the optimal control of geometric evolution laws. Journal of Computational Physics, 2015, 297, 495-514.	3.8	9
41	Automatic segmentation of focal adhesions from mouse embryonic fibroblasts. , 2015, , .		Ο
42	A Robust and Artifact Resistant Algorithm of Ultrawideband Imaging System for Breast Cancer Detection. IEEE Transactions on Biomedical Engineering, 2015, 62, 1514-1525.	4.2	53
43	Microfluidic environment and tracking analysis for the observation of Artemia Franciscana. , 2015, , .		2
44	Tumour Cells Expressing Single VEGF Isoforms Display Distinct Growth, Survival and Migration Characteristics. PLoS ONE, 2014, 9, e104015.	2.5	14
45	An <i>in vivo</i> role for <scp>R</scp> ho kinase activation in the tumour vascular disrupting activity of combretastatin <scp>A</scp> â€4 3â€ <scp><i>O</i></scp> â€phosphate. British Journal of Pharmacology, 2014, 171, 4902-4913.	5.4	14
46	Homage to Professor Maria Petrou. Pattern Recognition Letters, 2014, 48, 2-7.	4.2	1
47	Influence of soluble or matrix-bound isoforms of vascular endothelial growth factor-A on tumor response to vascular-targeted strategies. International Journal of Cancer, 2013, 133, n/a-n/a.	5.1	11
48	Cxcl8 (IL-8) Mediates Neutrophil Recruitment and Behavior in the Zebrafish Inflammatory Response. Journal of Immunology, 2013, 190, 4349-4359.	0.8	294
49	PhagoSight: An Open-Source MATLAB® Package for the Analysis of Fluorescent Neutrophil and Macrophage Migration in a Zebrafish Model. PLoS ONE, 2013, 8, e72636.	2.5	41
50	Drift-Diffusion Analysis of Neutrophil Migration during Inflammation Resolution in a Zebrafish Model. Advances in Hematology, 2012, 2012, 1-8.	1.0	29
51	Local affine texture tracking for serial registration of zebrafish images. , 2012, , .		1
52	Repelled from the wound, or randomly dispersed? Reverse migration behaviour of neutrophils characterized by dynamic modelling. Journal of the Royal Society Interface, 2012, 9, 3229-3239.	3.4	55
53	Neutrophil-Delivered Myeloperoxidase Dampens the Hydrogen Peroxide Burst after Tissue Wounding in Zebrafish. Current Biology, 2012, 22, 1818-1824.	3.9	117
54	Online chromatic and scale-space microvessel-tracing analysis for transmitted light optical images. Microvascular Research, 2012, 84, 330-339.	2.5	5

#	Article	IF	CITATIONS
55	The Neutrophil's Eye-View: Inference and Visualisation of the Chemoattractant Field Driving Cell Chemotaxis In Vivo. PLoS ONE, 2012, 7, e35182.	2.5	17
56	Activation of hypoxia-inducible factor- $1\hat{l}$ (Hif- $1\hat{l}$) delays inflammation resolution by reducing neutrophil apoptosis and reverse migration in a zebrafish inflammation model. Blood, 2011, 118, 712-722.	1.4	218
57	An automatic algorithm for the segmentation and morphological analysis of microvessels in immunostained histological tumour sections. Journal of Microscopy, 2011, 242, 262-278.	1.8	53
58	CAIMAN: An online algorithm repository for Cancer Image Analysis. Computer Methods and Programs in Biomedicine, 2011, 103, 97-103.	4.7	15
59	Vascular effects dominate solid tumor response to treatment with combretastatin Aâ€4â€phosphate. International Journal of Cancer, 2011, 129, 1979-1989.	5.1	32
60	Microflow of fluorescently labelled red blood cells in tumours expressing single isoforms of VEGF and their response to vascular targeting agents. Medical Engineering and Physics, 2011, 33, 805-809.	1.7	3
61	Application of intravital microscopy in studies of tumor microcirculation. Journal of Biomedical Optics, 2010, 15, 011113.	2.6	25
62	Retrospective shading correction algorithm based on signal envelope estimation. Electronics Letters, 2009, 45, 454.	1.0	24
63	Estimation of Apparent Tumor Vascular Permeability from Multiphoton Fluorescence Microscopic Images of P22 Rat Sarcomas In Vivo. Microcirculation, 2008, 15, 65-79.	1.8	51
64	Measuring the velocity of fluorescently labelled red blood cells with a keyhole tracking algorithm. Journal of Microscopy, 2008, 229, 162-173.	1.8	37
65	Blood Vessel Maturation and Response to Vascular-Disrupting Therapy in Single Vascular Endothelial Growth Factor-A Isoform–Producing Tumors. Cancer Research, 2008, 68, 2301-2311.	0.9	92
66	Measuring cellular migration with image processing. Electronics Letters, 2008, 44, 791.	1.0	6
67	Measuring Red Blood Cell Velocity with a Keyhole Tracking Algorithm. , 2007, , 810-813.		1
68	The Bhattacharyya space for feature selection and its application to texture segmentation. Pattern Recognition, 2006, 39, 812-826.	8.1	82
69	Volumetric Texture Description and Discriminant Feature Selection for MRI. Lecture Notes in Computer Science, 2003, 18, 282-293.	1.3	15
70	A hybrid model based on dynamic programming, neural networks, and surrogate value for inventory optimisation applications. Journal of the Operational Research Society, 1999, 50, 85-94.	3.4	10
71	Volumetric Texture Analysis in Biomedical Imaging. Advances in Medical Technologies and Clinical Practice Book Series, 0, , 200-248.	0.3	3